Inorganic Chemistry

Article

pubs.acs.org/IC

Copper(II) Coordination Polymers Self-Assembled from Aminoalcohols and Pyromellitic Acid: Highly Active Precatalysts for the Mild Water-Promoted Oxidation of Alkanes

Tiago A. Fernandes,[†] Carla I. M. Santos,[†] Vânia André,[†] Julia Kłak,[‡] Marina V. Kirillova,*[,†] and Alexander M. Kirillov*[,†]

[†]Centro de Química Estrutural, Complexo I, Instituto Superior Técnico, Universidade de Lisboa, Av. Rovisco Pais, 1049-001, Lisbon, Portugal

[‡]Faculty of Chemistry, University of Wrocław, ul. F. Joliot-Curie 14, 50-383 Wrocław, Poland

Supporting Information

ABSTRACT: Three novel water-soluble 2D copper(II) coordination polymers—$[\{Cu_2(\mu_2\text{-dmea})_2(H_2O)\}_2(\mu_4\text{-pma})]_n\cdot 4nH_2O$ (**1**), $[\{Cu_2(\mu_2\text{-Hedea})_2\}_2(\mu_4\text{-pma})]_n\cdot 4nH_2O$ (**2**), and $[\{Cu(bea)(Hbea)\}_4(\mu_4\text{-pma})]_n\cdot 2nH_2O$ (**3**)—were generated by an aqueous medium self-assembly method from copper(II) nitrate, pyromellitic acid (H_4pma), and different aminoalcohols [*N*,*N*-dimethylethanolamine (Hdmea), *N*-ethyldiethanolamine (H_2edea), and *N*-benzylethanolamine (Hbea)]. Compounds **2** and **3** represent the first coordination polymers derived from H_2edea and Hbea. All the products were characterized by infrared (IR), electron paramagnetic resonance (EPR), and ultraviolet−visible light (UV-vis) spectroscopy, electrospray ionization−mass spectroscopy (ESI-MS(±)), thermogravimetric and elemental analysis, and single-crystal X-ray diffraction (XRD), which revealed that their two-dimensional (2D) metal−organic networks are composed of distinct dicopper(II) or monocopper(II) aminoalcoholate units and μ_4-pyromellitate spacers. From the topological viewpoint, the underlying 2D nets of **1**−**3** can be classified as uninodal 4-connected layers with the **sql** topology. The structures of **1** and **2** are further extended by multiple intermolecular hydrogen bonds, resulting in three-dimensional (3D) hydrogen-bonded networks with rare or unique topologies. The obtained compounds also act as highly efficient precatalysts for the mild homogeneous oxidation, by aqueous H_2O_2 in acidic MeCN/H_2O medium, of various cycloalkanes to the corresponding alcohols and ketones. Overall product yields up to 45% (based on cycloalkane) were attained and the effects of various reaction parameters were investigated, including the type of precatalyst and acid promoter, influence of water, and substrate scope. Although water usually strongly inhibits the alkane oxidations, a very pronounced promoting behavior of H_2O was detected when using the precatalyst **1**, resulting in a 15-fold growth of an initial reaction rate in the cyclohexane oxidation on increasing the amount of H_2O from ∼4 M to 17 M in the reaction mixture, followed by a 2-fold product yield growth.

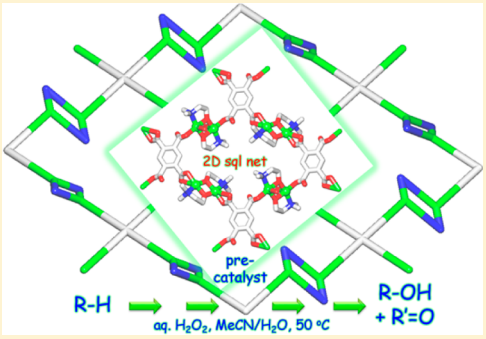

INTRODUCTION

Within the sweeping progress of research on the design, synthesis, and properties of metal−organic networks,[1] water-soluble coordination polymers (CPs) represent a significantly less explored class of compounds which, however, possess a diversity of notable applications in modern chemistry. In particular, bioactive and/or biomimetic CPs[2] have found significance in the fields of drug delivery and antimicrobial treatment, selective sorption, and homogeneous bioinspired catalysis.[3,4] The solubility of CPs in aqueous medium can be achieved by introducing into the structure at least one organic building block that is soluble in water. Aminoalcohols are particularly attractive examples of such building blocks, because of their coordination flexibility and versatility, low toxicity and bioactivity, as well as high stability, solubility, and low cost.[5]

Although a few common aminoalcohols (e.g., diethanolamine and triethanolamine) have been well-explored for the synthesis of metal−organic networks,[6] there are some simple and commercially available aminoalcohol building blocks that have never been applied toward the design of CPs. For example, a search of the Cambridge Structural Database (CSD) reveals no examples of coordination polymers derived from *N*-ethyldiethanolamine (H_2edea) and *N*-benzylethanolamine (Hbea),[6] while their coordination chemistry is limited to a few discrete metal complexes.[7] Considering the above-mentioned points and following our general interest in exploring various aminoalcohol building blocks for the generation of multicopper(II) cores and coordination polymers with significance in aqueous-medium catalysis, molecular magnetism, and supramolecular chemistry,[8] the principal objectives of the current study were as follows:

Received: August 27, 2015

DOI: 10.1021/acs.inorgchem.5b01983
Inorg. Chem. XXXX, XXX, XXX−XXX

(1) To probe diverse aminoalcohol ligands for the preparation of novel mixed-ligand copper(II) CPs that would potentially show solubility in water.
(2) To verify whether a slight variation of the type of aminoalcohol block would alter the structural features and properties of coordination polymers derived from a common organic linker: pyromellitic acid (H_4pma).
(3) To test the obtained products as water-soluble precatalysts in the mild homogeneous oxidation of alkanes.

Thus, in the present study, we report a simple aqueous medium self-assembly synthesis, full characterization, structural and topological features, and catalytic properties of three novel, water-soluble and mixed-ligand two-dimensional (2D) copper(II) coordination polymers—$[\{Cu_2(\mu_2\text{-dmea})_2(H_2O)\}_2(\mu_4\text{-pma})]_n\cdot 4nH_2O$ (**1**), $[\{Cu_2(\mu_2\text{-Hedea})_2\}_2(\mu_4\text{-pma})]_n\cdot 4nH_2O$ (**2**), and $[\{Cu(bea)(Hbea)\}_4(\mu_4\text{-pma})]_n\cdot 2nH_2O$ (**3**)—which were assembled from rigid pyromellitic acid linkers and different flexible aminoalcohol building blocks (Scheme 1).

Scheme 1. Structural Formulae of Organic Building Blocks

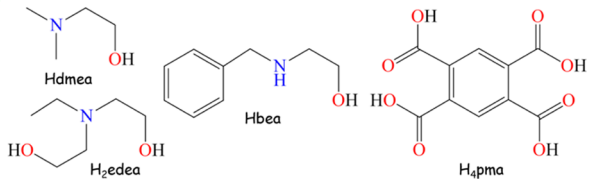

The latter vary in sterical hindrance, number of ethanolamine arms, and presence of different *N*-aliphatic (methyl, ethyl) or *N*-aromatic (benzyl) groups. Apart from representing the first coordination polymers derived from H_2edea (compound **2**) and Hbea (compound **3**), all of the obtained products (**1**–**3**) also act as highly efficient precatalysts for the mild oxidation of different alkanes to alcohols and ketones, by H_2O_2 and in aqueous acidic MeCN medium, revealing a very unusual promoting role of water.

EXPERIMENTAL SECTION

Self-Assembly Synthesis and Characterization. *$[\{Cu_2(\mu_2\text{-dmea})_2(H_2O)\}_2(\mu_4\text{-pma})]_n\cdot 4nH_2O$ (**1**).* An excess of *N*,*N*′-dimethylethanolamine (Hdmea; 5.0 mmol, 0.50 mL) and pyromellitic acid (0.50 mmol, 127 mg) were added in this order, to an aqueous solution (10 mL) containing $Cu(NO_3)_2\cdot 2.5H_2O$ (1.00 mmol, 233 mg) and with continuous stirring at room temperature. The resulting reaction mixture was stirred during 2 h and then filtered off. The filtrate was left to evaporate in a beaker at ambient temperature. Blue X-ray-quality crystals were formed within 2–3 weeks, then collected and dried in air to furnish compound **1** in ∼60% yield (based on copper(II) nitrate). Compound **1** is very soluble in H_2O ($S_{25\,°C}$ > 15 mg mL^{-1}). Anal. Calcd (%) for **1**–H_2O, $C_{26}H_{52}Cu_4N_4O_{17}$: C 32.98, H 5.54, N 5.92; found C 33.09, H 5.48, N 6.30. FT-IR (KBr): 3453 (s br), 3408 (s), and 3276 (sh) ν(H_2O), 2970 (w), 2878 (w), and 2851 (w) ν(CH), 1669 (s), 1612 (s) and 1601 (s, one broad band with two maxima) ν_{as}(COO), 1489 (m), 1468 (m), 1405 (s) and 1385 (s) and 1355 (s) ν_s(COO), 1281 (m), 1131 (s), 1090 (m), 1066 (m), 1018 (w), 950 (w), 868 (w), 826 (w), 785 (w), 656 (m), 562 (w), 530 (w), and 473 (w) cm^{-1}. ESI–MS(±) (H_2O), selected fragments: MS(+), *m*/*z*: 977 $[Cu_5(Hdmea)_4(pma)(H_2O)_3]^+$, 797 $[Cu_3(Hdmea)_4(pma)]^+$; MS(−), *m*/*z*: 1109 $[Cu_4(dmea)_4(pma)(H_3pma)]^-$, 929 $[Cu_4(dmea)_4(pma)(H_2O)_4]^-$, 554 $[Cu_2(Hdmea)_2(pma)]^-$, 377 $[Cu_2(pma)]^-$, 315 $[Cu(Hpma)]^-$, 253 $[H_3pma]^-$. TGA (N_2, 5 °C/min): 50–180 °C (−4H_2O; Δ*m*: 7.3% expt., 7.5% calcd.), 180–260 °C (−2H_2O, decomposition of dmea), 260–370 °C (decomposition of pma, formation of CuO; total Δ*m*: 66.3% expt., 67.0% calcd.).

*$[\{Cu_2(\mu_2\text{-Hedea})_2\}_2(\mu_4\text{-pma})]_n\cdot 4nH_2O$ (**2**).* This product was obtained following the procedure described for **1**, but using a mixture of *N*-ethyldiethanolamine (H_2edea; 2.0 mmol, 525 μL) and KOH (3.00 mmol, 3 mL, 1 M aqueous solution) instead of Hdmea. Dark-blue X-ray-quality crystals of **2** were obtained in ∼50% yield (based on copper(II) nitrate). Compound **2** is barely soluble in H_2O ($S_{25\,°C}$ ≈ 1 mg mL^{-1}). Anal. Calcd (%) for **2**+H_2O, $C_{34}H_{68}Cu_4N_4O_{21}$: C 36.36, H 6.10, N 4.99; found C 36.49, H 6.18, N 4.82. FT-IR (KBr): 3418 (s br) ν(H_2O), 2978 (w), 2859 (w) and 2845 (m) ν(CH), 1611 (s br) ν_{as}(COO), 1492 (w), 1467 (w), 1406 (s) and 1362 (s) and 1333 (sh) ν_s(COO), 1247 (w), 1139 (s), 1072 (s), 1042 (m), 1028 (w), 920 (w), 897 (w), 815 (w), 752 (w), 618 (w), 571 (w), and 512 (w) cm^{-1}. ESI–MS(±) (H_2O), selected fragments: MS(+), *m*/*z*: 1032 $[Cu_4(Hedea)_4(Hpma)]^+$, 839 $[Cu_3(Hedea)_3(H_2pma)]^+$, 643 $[Cu_2(Hedea)_2(H_3pma)]^+$, 134 $[H_2edea + H]^+$; MS(−), *m*/*z*: 1019 $[Cu_4(Hedea)_2(pma)\ (Hpma)]^-$, 641 $[Cu_2(Hedea)_2(Hpma)]^-$, 507 $[Cu_2(Hedea)\ (pma)]^-$, 253 $[H_3pma]^-$. TGA (N_2, 5 °C/min): 60–170 °C (−4H_2O; Δ*m*: 5.8% expt., 6.5% calcd.), 170–350 °C (decomposition of Hedea), 350–500 °C (decomposition of pma, formation of CuO; total Δ*m*: 68.1% expt., 71.2% calcd.).

*$[\{Cu(bea)(Hbea)\}_4(\mu_4\text{-pma})]_n\cdot 2nH_2O$ (**3**).* This product was obtained by following the procedure described for **1**, but using a mixture of *N*-benzylethanolamine (Hbea; 5.0 mmol, 710 μL) and KOH (3.00 mmol, 3 mL, 1 M aqueous solution) instead of Hdmea. Light-blue X-ray-quality crystals of **3** were obtained in ∼60% yield (based on copper(II) nitrate). Compound **3** is soluble in H_2O ($S_{25\,°C}$ ≈ 4 mg mL^{-1}). Anal. Calcd (%) for **3**+NO_3, $C_{82}H_{106}Cu_4N_9O_{21}$: C 54.47, H 5.91, N 6.97; found C 54.37, H 5.72, N 6.56. FT-IR (KBr): 3231 (s) and 3184 (s) ν(H_2O) + ν(NH), 2940 (w), 2885 (w), and 2829 (w) ν(CH), 1454 (s) ν_{as}(COO), 1393 (sh) and 1365 (vs br) and 1319 (sh) ν_s(COO), 1250 (w), 1076 (m), 1049 (m), 1039 (m), 1015 (w), 970 (w), 943 (w), 902 (w), 827 (w), 754 (s), 702 (s), 641 (w), 596 (w), 534 (w), 458 (w), and 431 (w) cm^{-1}. ESI–MS(±) (H_2O), selected fragments: MS(+), *m*/*z*: 152 $[Hbea + H]^+$; MS(−), *m*/*z*: 679 $[Cu(Hbea)_2(pma)]^-$, 363 $[Cu(bea)_2 - H]^-$, 253 $[H_3pma]^-$. TGA (N_2, 5 °C/min): 50–110 °C (−2H_2O; Δ*m*: 2.4% expt., 2.1% calcd.), 200–415 °C (decomposition of bea/Hbea), 415–520 °C (decomposition of pma, formation of CuO; total Δ*m*: 83.0% expt., 81.8% calcd.).

X-ray Crystallography. Crystals of **1**–**3** suitable for X-ray diffraction (XRD) study were mounted with Fomblin in a cryoloop. Data were collected on a Bruker AXS-KAPPA APEX II diffractometer with graphite-monochromated radiation (Mo Kα, λ = 0.17073 Å) at 298 K. The X-ray generator was operated at 50 kV and 30 mA and the X-ray data collection was monitored by the APEX2[9] program. All data were corrected for Lorentzian, polarization, and absorption effects, using SAINT[9] and SADABS[9] programs. SIR-97[10] and SHELXS-97[11] were used for structure solution and SHELXL-97[11] was applied for full matrix least-squares refinement on F^2. These three programs are included in the package of programs WINGX-Version 1.80.05.[12] Non-hydrogen atoms were refined anisotropically. A full-matrix least-squares refinement was used for the non-hydrogen atoms with anisotropic thermal parameters. All the H atoms were inserted in idealized positions and allowed to refine in the parent C or O atom. TOPOS 4.0[13] and PLATON[14] were applied for topological analysis and hydrogen bond interactions, respectively. Crystal data and details of the data collection for **1**–**3** are reported in Table 1.

Catalytic Studies. The alkane oxidations were typically carried out in an air atmosphere in thermostated glass reactors equipped with a condenser under vigorous stirring and using MeCN as the solvent (up to a total volume of 2.5 mL) at 50 °C. In a typical experiment, precatalyst **1**–**3** (5×10^{-3} mmol) and gas chromatography (GC) internal standard ($MeNO_2$, 25 μL) were introduced into a MeCN solution, followed by the addition of an acid promoter (0.05 mmol, optional) used as a stock solution in MeCN. The alkane substrate (1 mmol) was then introduced, and the reaction started upon addition of hydrogen peroxide (50% in H_2O, 5 mmol) in one portion. The reactions were monitored by withdrawing small aliquots after different

DOI: 10.1021/acs.inorgchem.5b01983
Inorg. Chem. XXXX, XXX, XXX–XXX

Table 1. Crystal Data and Structure Refinement Details for 1−3

	1	2	3
formula	$C_{13}H_{27}Cu_2N_2O_9$	$C_{17}H_{29}Cu_2N_2O_{10}$	$C_{23}H_{28}CuN_2O_7$
fw	482.44	548.50	508.01
crystal form, color	block, blue	block, blue	plate, blue
crystal size, mm	0.05 × 0.03 × 0.03	0.04 × 0.03 × 0.02	0.08 × 0.05 × 0.04
cryst. syst.	triclinic	monoclinic	triclinic
space group	$P\bar{1}$	$P2_1/c$	$P\bar{1}$
a, Å	8.5488(7)	13.0515(12)	10.9067(11)
b, Å	11.1202(9)	14.5150(14)	11.0800(12)
c, Å	12.2436(10)	12.6791(12)	11.1272(12)
α, deg	111.443(3)	90.00	83.799(4)
β, deg	107.668(3)	100.520(3)	85.737(4)
γ, deg	97.411(3)	90.00	65.227(2)
Z	2	4	2
V, Å^3	993.77(14)	2361.6(4)	1213.2(2)
T, K	293(2)	293(2)	293(2)
D_c, g cm^{-3}	1.612	1.543	1.391
μ(Mo Kα), mm^{-1}	2.185	1.853	0.944
θ range (deg)	2.597−25.242	2.492−25.242	2.624−31.102
no. of refl. collected	39065	27502	66251
no. of independent refl.	6778	4243	7776
R_{int}	0.1148	0.0882	0.0607
R_1[a], wR_2[b] [$I \geq 2\sigma(I)$]	0.0593, 0.1008	0.0933, 0.2240	0.0439, 0.0852
GOF on F^2	1.001	1.041	1.056

[a] $R_1 = \sum||F_0| - |F_c||/\sum|F_0|$. [b] $wR_2 = [\sum[w(F_0^2 - F_c^2)^2]/\sum[w(F_0^2)^2]]^{1/2}$.

periods of time, which were treated with PPh_3 (following a method developed by Shul'pin)[15] for reduction of remaining H_2O_2 and alkyl hydroperoxides that are typically formed as major primary products in alkane oxidations. The samples were analyzed by gas chromatography (GC), using nitromethane as an internal standard. Attribution of peaks was made by comparison with chromatograms of authentic samples. Chromatographic analyses were run on an Agilent Technologies 7820A series gas chromatograph (with helium as the carrier gas) equipped with the FID detector and BP20/SGE (30 m × 0.22 mm × 0.25 μm) capillary column. Blank tests confirmed that alkane oxidations do not proceed in the absence of copper precatalyst.

RESULTS AND DISCUSSION

Synthesis and Characterization. The 2D coordination polymers $[\{Cu_2(\mu_2\text{-dmea})_2(H_2O)\}_2(\mu_4\text{-pma})]_n\cdot 4nH_2O$ (**1**), $[\{Cu_2(\mu_2\text{-Hedea})_2\}_2(\mu_4\text{-pma})]_n\cdot 4nH_2O$ (**2**), and $[\{Cu(bea)(Hbea)\}_4(\mu_4\text{-pma})]_n\cdot 2nH_2O$ (**3**) were generated as microcrystalline solids by an aqueous medium self-assembly method. It is based on a simple combination, in water at ∼25 °C and in air, of $Cu(NO_3)_2\cdot 2.5H_2O$ with an aminoalcohol [*N*,*N*′-dimethylethanolamine (Hdmea), *N*-ethyldiethanolamine (H_2edea), or *N*-benzylethanolamine (Hbea) for **1**−**3**, respectively] as a main building block and pyromellitic acid (H_4pma) as a spacer or linker. An excess of aminoalcohol (for **1**−**3**) and additionally an aqueous solution of potassium hydroxide (for **2** and **3**) were required to maintain the basicity (pH 10−12) of the reaction mixtures. Compounds **1**−**3** were isolated as air-stable microcrystalline solids and characterized by IR, EPR and UV-vis spectroscopy, ESI-MS(±), thermogravimetric and elemental analysis, and single-crystal X-ray diffraction.

The selection of pyromellitic acid was governed by its recognized application as a linker in crystal engineering of copper(II)-organic networks.[16,17] Despite similar network dimensionality, compounds **1**−**3** are built from the structurally distinct dicopper(II) or monocopper(II) aminoalcoholate secondary building units (SBUs). Their self-assembly appeared to be primarily guided by the type of aminoalcohol building block, which also influences the solubility of the resulting product in H_2O. In fact, water solubility values vary from ∼1 mg mL^{-1} for a barely soluble **2** to ∼4 mg mL^{-1} for **3**, and >15 mg mL^{-1} for a well-soluble product **1**. Compounds **1**−**3** can partially dissociate upon dissolution in water, as confirmed by the ESI-MS(±) data, revealing the presence of heaviest fragments derived from molecular units, namely, $[Cu_5(Hdmea)_4(pma)(H_2O)_3]^+$ (m/z = 977) and $[Cu_4(dmea)_4(pma)(H_2O)_4]^-$ (m/z = 929) for **1**, $[Cu_4(Hedea)_4(Hpma)]^+$ (m/z = 1032) and $[Cu_4(Hedea)_2(pma)(Hpma)]^-$ (m/z = 1019) for **2**, and $[Cu(Hbea)_2(pma)]^-$ (m/z = 679) for **3**. A relatively low intensity of these peaks in both positive and negative modes can be explained by the difficulty in fragmentation of polymeric networks, probably suggesting their stability in aqueous medium. In fact, the compounds can be recrystallized or self-assembled again after dissolution. However, the relative intensity of the ESI-MS(±) patterns of **1**−**3** increases upon an addition of a small amount of HNO_3, suggesting that an acidic medium promotes a partial disaggregation of these metal−organic networks.

The EPR spectra of powdered samples of **1** and **2** recorded in the X-band at 293 and 77 K are essentially similar and show a few poorly resolved lines (Figure S1 in the Supporting Information). These spectral shapes can be compatible with the presence of magnetically nonequivalent copper(II) centers in the ligand fields of the distorted square-pyramidal geometries.[18−20] Moreover, in a low field part of the spectrum (at 1500 G), there is one ΔM_S = 2 transition that confirms an exchange interaction between metal atoms in dicopper(II) blocks. The EPR data of **3** are typical for copper(II) centers in a ligand field of the distorted octahedral $\{CuN_2O_4\}$ symmetry.[18−20] Only a broad isotropic signal with the g value of ∼2.14 was observed. The UV−vis spectra of solid samples **1**−**3** display absorptions both in the UV and visible regions (Figure S2 in the Supporting Information). The strong absorption bands near 330 and 360 nm are due to $\pi \rightarrow \pi^*$ and n $\rightarrow \pi^*$ transitions of ligands. The broad bands in the visible region are due to d−d transitions. Five-coordinated copper(II) compounds with *O*-donor ligands usually have[18,21] two absorption bands lying near 1220 and 980 nm. The spectra of **1** and **2** are very similar, being consistent with a small difference in ligand field. They both display a very broad d−d band at 850 nm. Six-coordinated compounds typically give rise to one absorption band in the visible region[18,21] and the peak near 700 nm is observed in **3**.

The thermogravimetric analyses (TGA) of **1**−**3** show a series of typical thermal effects corresponding to a removal of crystallization water molecules and a stepwise decomposition of metal−organic networks (see Figures S3−S5 in the Supporting Information). For example, four crystallization H_2O molecules of **1** are released in the 50−180 °C range, whereas a next more-complex thermal effect in the 180−260 °C temperature interval corresponds to the removal of two water ligands along with the decomposition of dmea moieties. Further heating up to 370 °C

DOI: 10.1021/acs.inorgchem.5b01983
Inorg. Chem. XXXX, XXX, XXX−XXX

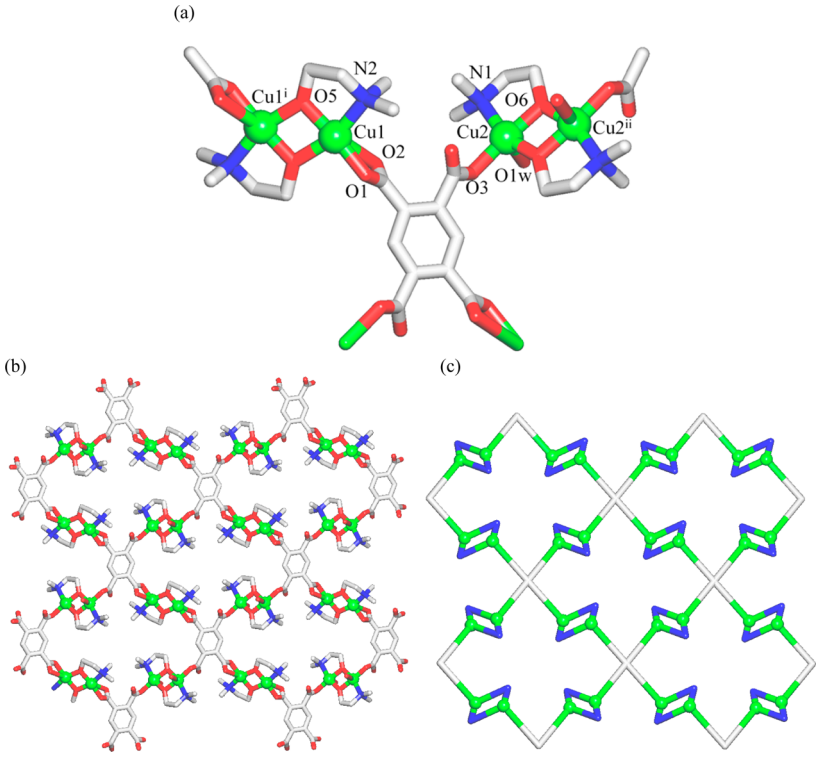

Figure 1. Structural fragments of **1** showing (a) interlinkage of two distinct dicopper(II) $[Cu_2(\mu_2\text{-dmea})_2]^{2+}$ and $[Cu_2(\mu_2\text{-dmea})_2(H_2O)_2]^{2+}$ units, (b) 2D metal−organic layer, and (c) its topological representation displaying a uninodal 4-connected underlying net with the **sql** topology. Further details: (panels a and b) H atoms and crystallization H_2O molecules are omitted for clarity, Cu (green), O (red), N (blue), and C (gray); (c) terminal H_2O ligands were omitted for clarity; Cu centers (green), centroids of μ_2-dmea (blue) and μ_4-pma (gray) blocks. Symmetry codes: (a): (i) $-x+1, -y+1, -z+2$; (ii) $-x+1, -y+2, -z+1$. Selected distances (Å): Cu1−N2, 2.018(4); Cu1−O1, 1.919(4); Cu1−O2, 2.713(3); Cu1−O5, 1.920(3); $Cu1^i$−O5, 1.886(4); Cu1···$Cu1^i$, 2.9763(8); Cu2−N1, 2.009(4); Cu2−O1w, 2.337(6); Cu2−O3, 1.940(2); Cu2−O6, 1.918(4); $Cu2^{ii}$−O6, 1.906(4); Cu2···$Cu2^i$, 2.9561(9).

leads to the decomposition of pma linkers. In contrast, the TGA pattern of **2** is shifted to higher temperatures, with the major thermal effects due to the loss of four crystallization H_2O molecules (60−170 °C), decomposition of Hedea (170−350 °C) and pma (350−500 °C) ligands. Similarly, the TGA pattern of **3** shows the removal of two crystallization H_2O molecules (50−110 °C) and the decomposition of bea/Hbea (200−415 °C) and pma (415−520 °C) moieties. The observed total weight loss in all samples **1**−**3** (Δm of 66.3%, 68.1%, and 83.0%, respectively) is very close to the calculated values assuming the formation of CuO residue.

Structural and Topological Description. The crystal structure of the 2D coordination polymer $[\{Cu_2(\mu_2\text{-dmea})_2(H_2O)\}_2(\mu_4\text{-pma})]_n{\cdot}4nH_2O$ (**1**) is composed of two distinct types of dicopper(II) $[Cu_2(\mu_2\text{-dmea})_2]^{2+}$ and $[Cu_2(\mu_2\text{-dmea})_2(H_2O)_2]^{2+}$ blocks (based on Cu1 and Cu2 centers, respectively), a μ_4-pma(4−) spacer, and four crystallization water molecules (Figure 1). The Cu1 atoms reveal a distorted $\{CuNO_4\}$ square-pyramidal environment (τ_5 = 0.21; this value is zero for an ideal square-pyramidal geometry),[22] filled by the N2, O5, and $O5^i$ atoms of bidentate μ_2-dmea ligands [Cu1−N2 2.018(4), Cu1−O5 1.919(4), Cu1−$O5^i$ 1.886(4) Å] and the O1 atom of μ_4-pma [Cu1−O1 1.920(3) Å] in equatorial sites, whereas the axial position is occupied by a weakly bound O2 carboxylate atom [Cu1−O2 2.713(3) Å] (Figure 1a). The Cu2 atoms also adopt a distorted $\{CuNO_4\}$ square-pyramidal environment (τ_5 = 0.29), formed by the aminoalcoholate N2, O6, and $O6^{ii}$ and carboxylate O3 atoms [Cu2−N1, 2.009(4); Cu2−O6, 1.918(4); Cu2−$O6^{ii}$, 1.906(4); Cu2−O3, 1.940(2) Å] in equatorial positions, while an axial site is taken by the terminal O1w water ligand [Cu2−O1w 2.337(6) Å]. In both types of the dicopper(II) blocks, the $\{Cu_2(\mu\text{-O})_2\}$ cores are planar and possess rather short Cu1 ···$Cu1^i$ [2.9763(9) Å] and Cu2···$Cu2^i$ [2.9561(9) Å] separations, with the corresponding Cu1−O5−$Cu1^i$ and Cu2−O6−$Cu2^{ii}$ angles of 102.92(14) and 101.23(12)°, respectively. The μ_4-pma(4−) moieties bear two pairs of distinct $\eta^1{:}\eta^1$- and $\eta^1{:}\eta^0$−COO groups that interlink the adjacent dicopper(II) aminoalcoholate blocks into a 2D metal−organic layer (see Figures 1b and 1c).

Similar to **1**, the structure of $[\{Cu_2(\mu_2\text{-Hedea})_2\}_2(\mu_4\text{-pma})]_n{\cdot}4nH_2O$ (**2**) also features a resembling 2D metal−organic network assembled from the $[Cu_2(\mu_2\text{-Hedea})_2]^{2+}$ and μ_4-pma(4−) blocks (see Figure S6 in the Supporting Information), and thus is not discussed in detail. The structural difference between **1** and **2** mainly concerns the absence in **2** of H_2O ligands and the presence of only one $\eta^1{:}\eta^0$−COO mode of carboxylate groups in μ_4-pma. The bonding parameters in **1** and **2** are comparable to those of other copper(II) compounds bearing dmea,[6,8c] Hedea,[7a,b] or pyromellitate[16,17] moieties. Besides, compound **2** represents the first coordination polymer derived from *N*-ethyldiethanolamine.[6]

Although the compound $[\{Cu(bea)(Hbea)\}_4(\mu_4\text{-pma})]_n{\cdot}2nH_2O$ (**3**) also discloses a 2D metal−organic network, it is however assembled from the monocopper(II) $[Cu(bae)_2]$ and $[Cu(Hbea)_2]^{2+}$ blocks (based on Cu1 and Cu2 centers, respectively) and μ_4-pma(4−) spacers (Figure 2). In contrast to five-coordinate Cu atoms and $\{CuNO_4\}$ environments in **1** and **2**, coordination polymer **3** possesses the six-coordinated

DOI: 10.1021/acs.inorgchem.5b01983
Inorg. Chem. XXXX, XXX, XXX−XXX

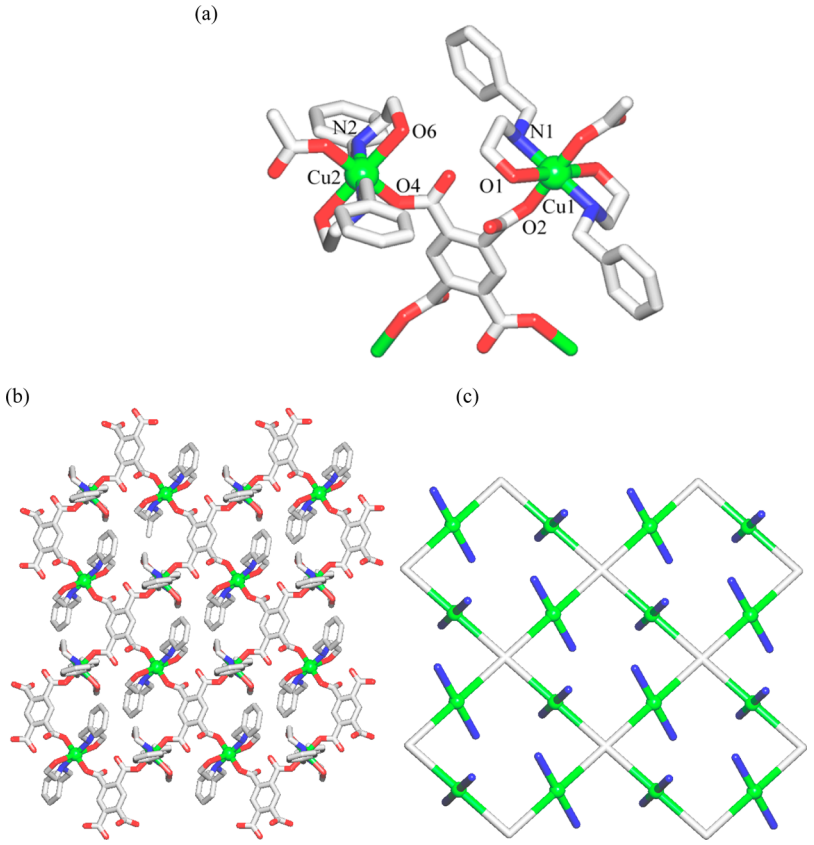

Figure 2. Structural fragments of **3** showing (a) interlinkage of two distinct monocopper(II) $[Cu(bea)_2]$ and $[Cu(Hbea)_2]^{2+}$ units, (b) 2D metal−organic layer, and (c) its topological representation displaying a uninodal 4-connected underlying net with the **sql** topology. Further details: (a, b) H atoms and crystallization H_2O molecules are omitted for clarity, Cu (green), O (red), N (blue), and C (gray); (c) Cu centers (green), centroids of bea/Hbea (blue) and μ_4-pma (gray) blocks. Selected distances (Å): Cu1−N1, 2.039(2); Cu1−O1, 2.583(2); Cu1−O2, 1.9546(13); Cu2−N2, 2.040(2); Cu2−O4, 1.9583(13); Cu2−O6, 2.4068(16).

Cu centers with a $\{CuN_2O_4\}$ octahedral geometry. Hence, the Cu1 atoms are surrounded by symmetry equivalent pairs of the N1 and O1 (from bea) and O2 (from μ_4-pma) atoms in a slightly distorted octahedral fashion [Cu1−N1, 2.039(2) Å; Cu1−O1, 2.583(2) Å; Cu1−O2, 1.9546(13) Å], wherein two aminoalcoholate O1 atoms occupy the axial sites. Similarly, the Cu2 centers bind the symmetry equivalent pairs of N2 and O6 atoms from Hbea and the O4 atoms from μ_4-pma [Cu2−N2, 2.040(2) Å; Cu2−O4, 1.9583(13) Å; Cu2−O6, 2.4068(16) Å]. As in **2**, the μ_4-pma(4−) spacers in **3** interlink the adjacent monocopper(II) units via four $\eta^1{:}\eta^0$−COO groups, resulting in a 2D metal−organic layer (Figures 2b and 2c) with the shortest Cu1···Cu1, Cu1···Cu2, and Cu2···Cu2 separations through μ_4-pma of 11.127(2), 7.415(2) (8.265(2)), and 11.080(2) Å, respectively. To our knowledge, compound **3** represents the first Cu coordination compound and the first coordination polymer (of any metal) derived from *N*-benzylethanolamine.[6]

Topological analysis of the 2D metal−organic networks in **1**−**3** was performed following the concept of the simplified underlying net;[13] such nets were generated by contracting all ligands to their centroids maintaining their connectivity (see Figures 1b and 2b). Despite being constructed from different dicopper(II) or monocopper(II) blocks, all the 2D underlying nets of **1**−**3** can be topologically classified as uninodal 4-connected layers with the **sql** [Shubnikov tetragonal plane net] topology and the point symbol of $(4^4.6^2)$.

Furthermore, the 2D metal−organic layers in **1** and **2** are further extended [2D → 3D], by means of multiple intermolecular hydrogen bonds and involving crystallization water molecules, to give very complex 3D supramolecular frameworks (see Figure S7 in the Supporting Information). To better understand the structures of these supramolecular nets, we carried out their topological analysis.[13,23] Hence, the hydrogen-bonded net of **1** was simplified by contracting dicopper(II) aminoalcoholate blocks, crystallization H_2O molecules, and pyromellitate spacers to their centroids, maintaining their connectivity via both coordination and hydrogen bonds; only conventional hydrogen bonds were considered [H···A < 2.50 Å, D···A < 3.50 Å, and ∠(D−H···A) > 120°; D and A stand for donor and acceptor atoms].[13] The resulting underlying net (Figure 3a) can be classified as a trinodal 3,4,8-connected framework with a rare **3,4,8T9** topology.[13] It is defined by the point symbol of $(3.4.5)_2(3^2.4^2.5^2.6^{14}.7^4.8^3.9)(3^2.6^3.7)$, wherein the notations $(3.4.5)$, $(3^2.4^2.5^2.6^{14}.7^4.8^3.9)$, and $(3^2.6^3.7)$ correspond to the 3-connected H_2O, 8-connected pma, and 4-connected $[Cu_2(\mu_2\text{-dmea})_2(H_2O)_2]^{2+}$ nodes, respectively; the $[Cu_2(\mu_2\text{-dmea})_2]^{2+}$ blocks act as the 2-connected linkers. Similarly, a three-dimensional (3D) hydrogen-bonded network of **2** was simplified and the obtained underlying framework (Figure 3b) was topologically classified as a trinodal 4,6,8-connected net. As confirmed by a search of various databases,[6,13,24] this net features the unique topology defined by the point symbol of $(3^2.4^2.5^2)_2(3^4.4^4.5^4.6^{15}.8)(3^4.4^4.5^4.6^3)$, wherein the $(3^2.4^2.5^2)$, $(3^4.4^4.5^4.6^{15}.8)$, and $(3^4.4^4.5^4.6^3)$ indices are those of the 4-connected $(H_2O)_2$ cluster nodes, 8-connected pma, and 6-

DOI: 10.1021/acs.inorgchem.5b01983
Inorg. Chem. XXXX, XXX, XXX−XXX

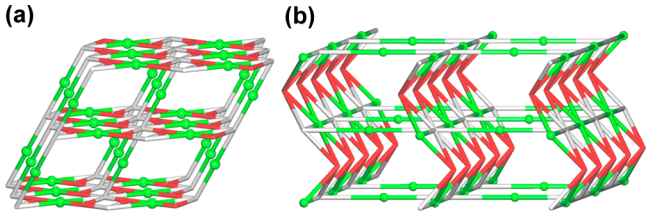

Figure 3. Topological representations of the underlying three-dimensional (3D) hydrogen-bonded frameworks in (a) **1** and (b) **2**. Panel (a) shows a trinodal 3,4,8-connected net with the **3,4,8T9** topology and point symbol of $(3.4.5)_2(3^2.4^2.5^2.6^{14}.7^4.8^3.9)(3^2.6^3.7)$, and panel (b) shows a trinodal 4,6,8-connected net in **2** with the unique topology and point symbol of $(3^2.4^2.5^2)_2(3^4.4^4.5^4.6^{15}.8)(3^4.4^4.5^4.6^3)$. Further details: (a) centroids of 2-connected $[Cu_2(\mu_2\text{-dmea})_2]^{2+}$ blocks and 4-connected $[Cu_2(\mu_2\text{-dmea})_2(H_2O)_2]^{2+}$ nodes (green), centroids of 3-connected H_2O nodes (red); (b) centroids of 2- and 6-connected $[Cu_2(\mu_2\text{-Hedea})_2]$ blocks (green), and centroids of 4-connected $(H_2O)_2$ nodes (red); (a, b) centroids of 8-connected pma nodes (gray).

connected $[Cu_2(\mu_2\text{-Hedea})_2]$ (based on Cu1 atoms) nodes, respectively; the $[Cu_2(\mu_2\text{-Hedea})_2]$ blocks based on the Cu2 atoms act the 2-connected linkers.

Mild Catalytic Oxidation of Alkanes. Although metal–organic networks are usually applied in heterogeneous catalysis, the coordination polymers that are soluble in aqueous and/or organic medium can act as precursors of catalytically active species in homogeneous catalytic systems.[25,26] Inspired by a solubility of compounds **1**–**3** in aqueous medium, we tested their catalytic activity toward the mild oxidation of cycloalkanes by aqueous H_2O_2 to give the corresponding alcohols and ketones. Cyclohexane was used as a model substrate[27] and typical oxidation reactions were carried out in aqueous acetonitrile medium, at 50 °C in air, and in the presence (optional) of an acid promoter.[25] It should be mentioned that the compounds **1**–**3** are not intact during the catalytic experiments and in the presence of an acid promoter and hydrogen peroxide lead to the formation of oligomeric catalytically active species, eventually via additional protonation and partial decoordination of aminoalcoholate or pyromellitate ligands.

All compounds showed a good activity under common reaction conditions with the total product yields of up to 36% based on cycloalkane (Table 2). The C_6H_{12} oxidation catalyzed by **1**–**3** in the presence of a small amount of trifluoroacetic acid (TFA) promoter (see Figure 4 for the accumulation of products with time) proceeds with the formation of cyclohexanol (main product) and cyclohexanone with their total yields of 24%, 30%, and 33%, respectively; for the detailed kinetic curves of product accumulation, see Figure S8 in the Supporting Information. In the absence of an acid promoter, **1** is inactive (Figure 5a), **2** shows modest activity (12% total yield, Figure S9 in the Supporting Information), while **3** reveals an appreciable total yield of 21% (Figure 5b) which is, however, inferior to that achieved in the presence of an acid promoter. The effect of different acid promoters was studied (see Figure 5, as well as Figure S9), revealing that the highest activity is observed in the systems containing TFA and HCl, followed by HNO_3, while H_2SO_4 is a less-active promoter. Following the literature background,[25,28−30] we believe that the acid promoter facilitates some proton transfer steps and activates the precatalysts by partial protonation of ligands and unsaturation of copper centers; it also improves the oxidation power of H_2O_2 and prevents its decomposition (e.g., catalase activity). In fact, a partial decomposition of H_2O_2 can be observed when using compound **1** in the absence of an acid promoter, thus explaining the very low yields that are observed in the oxidation of cyclohexane.

Table 2. Oxidation of Cycloalkanes by H_2O_2 in the Presence of Precatalysts 1−3[a]

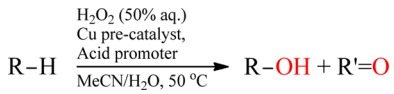

	Total Product Yield (Alcohol + Ketone) (%)[b]		
cycloalkane	1	2	3
C_5H_{10}	16.5	35.5	26.2
C_6H_{12}	23.9	29.8	32.5
C_7H_{14}	21.1	35.8	33.9
C_8H_{16}	25.7	35.5	31.6

[a]Reaction conditions: precatalyst **1**–**3** (0.005 mmol), acid promoter (TFA, 0.05 mmol), cycloalkane (1 mmol), H_2O_2 (50% aq. 5 mmol), CH_3CN (up to 2.5 mL of the total volume), 50 °C, 5 h. [b]Yields are based on alkanes [(mol of products per mol of cycloalkane) × 100%].

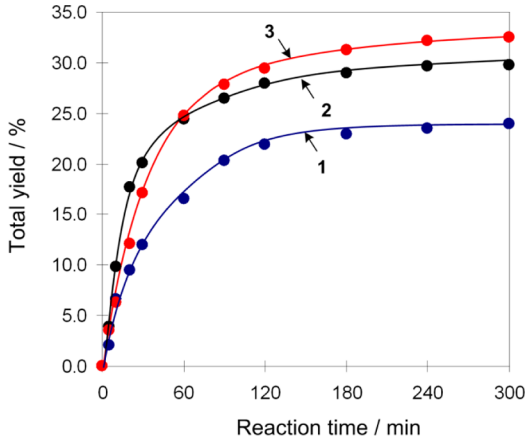

Figure 4. Accumulation of products (cyclohexanol and cyclohexanone, total yield, %) with time in the cyclohexane oxidation by H_2O_2 catalyzed by compounds **1**–**3** in the presence of TFA promoter. Reaction conditions: precatalyst **1**–**3** (0.005 mmol), TFA (0.05 mmol), C_6H_{12} (1.0 mmol), H_2O_2 (5.0 mmol), CH_3CN (up to 2.5 mL of the total volume), 50 °C.

In the presence of TFA, the reaction rate of the cyclohexane oxidation catalyzed by **1** is increased when the TFA concentration is increased up to 20 equiv, relative to the precatalyst amount (see Figure 6). After that, the initial reaction rate (W_0) is stabilized and is no longer dependent on the TFA concentration. The dependence of W_0 on the TFA amount has an S-shape, thus indicating second-order reaction kinetics, with respect to TFA. Hence, two TFA-containing species (or protons) are taking place in the rate-limiting step of the catalytic generation of hydroxyl radicals. Similar dependences of the total yield and initial reaction rate on the TFA amount were observed in the presence of compound **2** (Figure S10 in the Supporting Information). In contrast, an initial reaction rate of cyclohexane oxidation catalyzed by **3** has a linear dependence on the HNO_3 amount (Figure 7). The total yield is also rising, from 21% (in the absence of any acid promoter) to 36%, by increasing the amount of HNO_3 up to 20 equiv, relative to the

DOI: 10.1021/acs.inorgchem.5b01983
Inorg. Chem. XXXX, XXX, XXX−XXX

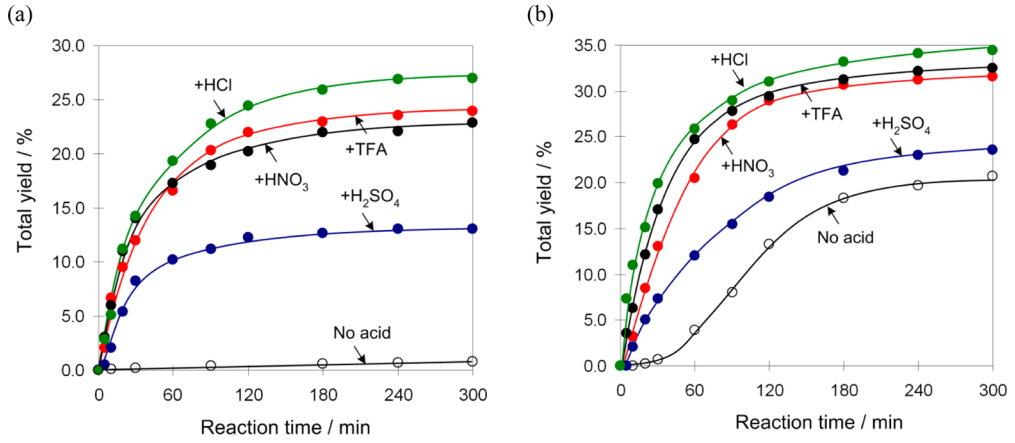

Figure 5. Effect of different acid promoters on the oxidation of cyclohexane catalyzed by (a) **1** and (b) **3**. Reaction conditions: precatalyst **1** or **3** (0.005 mmol), acid promoter (0.05 mmol), C_6H_{12} (1.0 mmol), H_2O_2 (5.0 mmol), CH_3CN (up to 2.5 mL of the total volume), 50 °C.

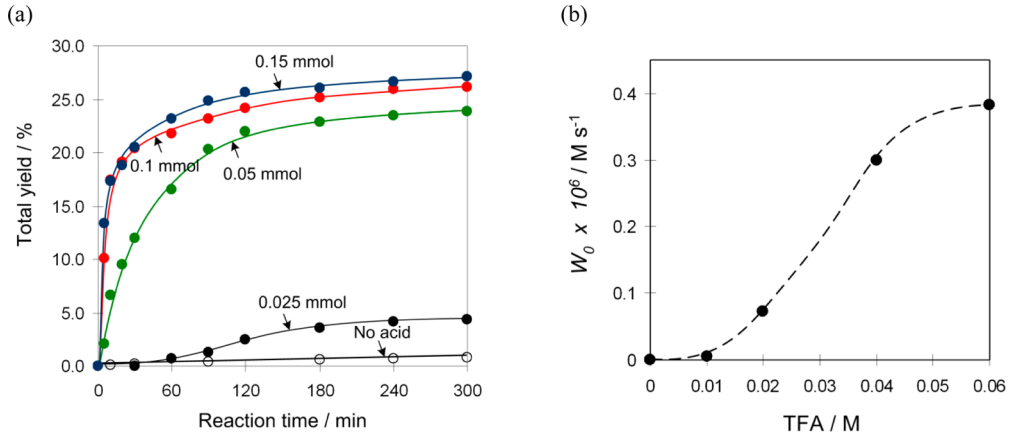

Figure 6. Effect of TFA amount on (a) the total yield of the products and (b) the maximum initial reaction rate (W_0) of the cyclohexane oxidation catalyzed by **1** in the presence of H_2O_2. Reaction conditions: precatalyst **1** (0.005 mmol), TFA (0.025–0.15 mmol), C_6H_{12} (1.0 mmol), H_2O_2 (5.0 mmol), CH_3CN (up to 2.5 mL of the total volume), 50 °C.

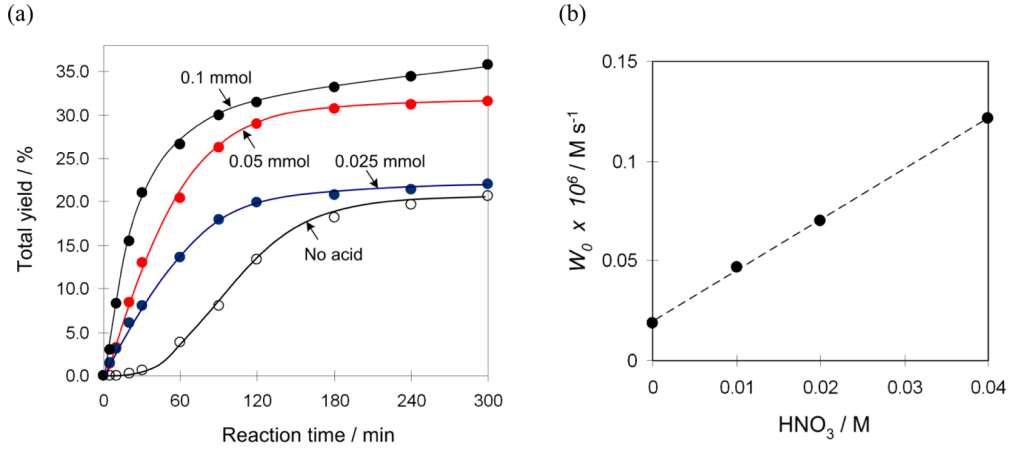

Figure 7. Effect of HNO_3 amount on (a) the total yield of the products and (b) the maximum initial reaction rate (W_0) of the cyclohexane oxidation catalyzed by **3** in the presence of H_2O_2. Reaction conditions: precatalyst **3** (0.005 mmol), HNO_3 (0.025–0.1 mmol), C_6H_{12} (1.0 mmol), H_2O_2 (5.0 mmol), CH_3CN (up to 2.5 mL of the total volume), 50 °C.

precatalyst. Besides, the increase of the acid promoter and water concentrations may also lead to higher extent of dissociation of the coordination polymers, generating catalytically active species of lower nuclearity, as confirmed by the ESI-MS tests.

The unusual promoting effect of water affecting both the total yield and reaction rate of cyclohexane oxidation was observed in the **1**/TFA/H_2O_2 system (Figure 8). The total yield of the products increases from 24% to 45% (Figure 8a) when increasing the water concentration in the system from 4 M (corresponding the amount of H_2O contained in 50%

DOI: 10.1021/acs.inorgchem.5b01983
Inorg. Chem. XXXX, XXX, XXX–XXX

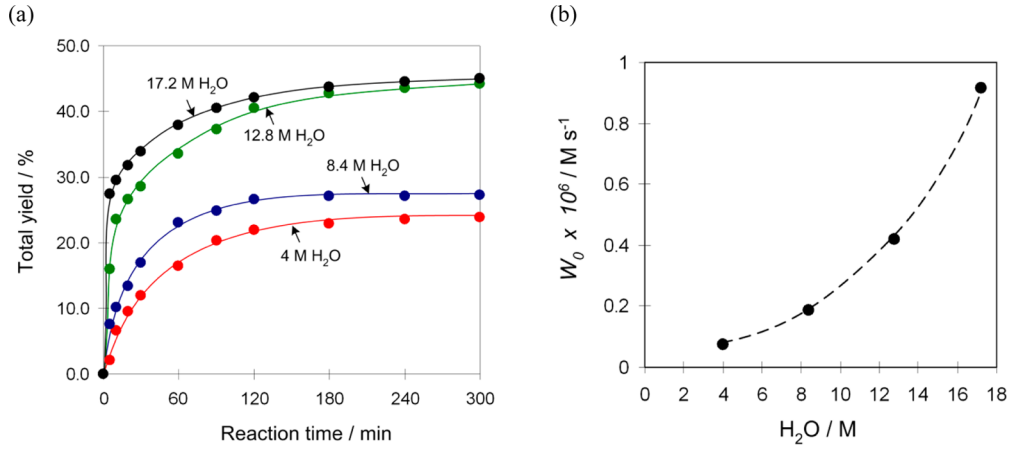

Figure 8. Effect of the amount of H_2O on (a) the total yield of the products and (b) the maximum initial reaction rate (W_0) of the cyclohexane oxidation catalyzed by **1**/TFA/H_2O_2 system. Reaction conditions: precatalyst **1** (0.005 mmol), TFA (0.05 mmol), C_6H_{12} (1.0 mmol), H_2O_2 (5.0 mmol), CH_3CN (up to 2.5 mL of the total volume), added H_2O (up to 0.6 mL), 50 °C.

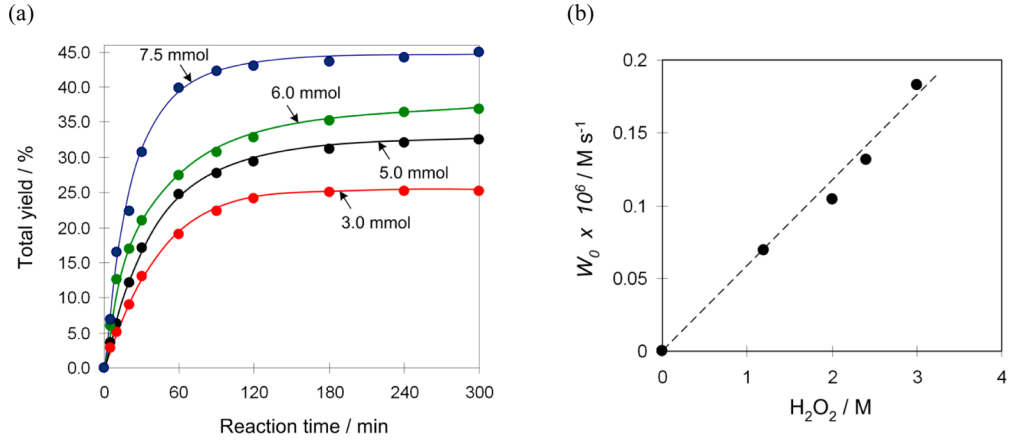

Figure 9. Effect of H_2O_2 amount on (a) the total yield of the products and (b) the maximum initial reaction rate (W_0) of the cyclohexane oxidation catalyzed by **3**/TFA/H_2O_2 system. Reaction conditions: precatalyst **3** (0.005 mmol), TFA (0.05 mmol), C_6H_{12} (1.0 mmol), H_2O_2 (3.0–7.5 mmol), CH_3CN (up to 2.5 mL of the total volume), 50 °C.

aqueous H_2O_2) to 17.2 M (after introduction of an additional amount of water to the reaction mixture). Besides, it is clearly seen from the dependence of the initial reaction rate (Figure 8b) that the addition of water dramatically accelerates the oxidation. Thus, we can conclude that there is a direct involvement of water in the rate-limiting step of catalytic generation of hydroxyl radicals. A similar behavior was earlier observed by us in the oxidation of alkanes catalyzed by a tetracopper(II) triethanolaminate derivative,[28b] as well as in the hydrocarboxylation reactions of alkanes that undergo only in a mixed H_2O/MeCN solvent.[26,31] Probably, in the present case, an additional amount of water helps to extend the catalytic life of the Cu-containing active species that most likely also bear some water ligands, as confirmed by the ESI-MS(±) investigation of the **1**/HNO_3/H_2O_2 system. Furthermore, a water-assisted mechanism for the generation of hydroxyl radicals in vanadium(V)- and rhenium(VII)-catalyzed alkane oxidation was earlier proposed based on the DFT calculations.[32]

The promoting role of water on the reaction rate of cyclohexane oxidation was also observed for the **2**/TFA/H_2O_2 system. However, in this case, the water accelerating effect is not so pronounced and does not alter the total product yield (Figure S11 in the Supporting Information). The W_0 exhibits a linear dependence on the H_2O concentration.

The H_2O_2 amount also has an influence on both the product yield and reaction rate of the cyclohexane oxidation. By rising the amount of hydrogen peroxide in the **3**/TFA/H_2O_2 system from 3.0 to 7.5 mmol, the total product yield is gradually increases from ~25% to 45% (Figure 9a), followed by a noticeable accelerating effect. Although the reaction rate linearly increases with hydrogen peroxide concentration (Figure 9b), there can also be an additional contribution due to the effect of water. The need for an excess of H_2O_2 relatively to the substrate to achieve higher yields of the oxidation products indicates that hydrogen peroxide also undergoes a partial catalytic decomposition, which is a common side reaction in Cu-catalyzed alkane oxidations.[4] Only traces of products were observed when *t*-BuOOH (70% in H_2O) was used instead of H_2O_2 under identical reaction conditions in the presence of all three precatalysts **1**–**3**, either with or without TFA promoter.

We have also studied the effect of catalyst amount on the reaction rate and total product yield of cyclohexane oxidation. For both compounds **1** and **2**, the linear dependence of W_0 on the precatalyst concentration in the presence of TFA promoter was found (see Figures S12 and S13 in the Supporting

DOI: 10.1021/acs.inorgchem.5b01983
Inorg. Chem. XXXX, XXX, XXX–XXX

Information), thus revealing the first-order reaction kinetics, which supports an involvement of one type of Cu-containing species in the rate-limiting catalytic step. The total yield of the products is also rising on increasing the precatalyst amount in the system, achieving the values of 26% and 36% when using 0.0075 mmol of compounds **1** and **2**, respectively.

It should be mentioned that the maximum overall product yields (up to 45% based on cyclohexane) obtained in the present study are superior to those achieved when using a variety of monocopper or dicopper complexes as homogeneous catalysts or precatalysts,[4,25,33a] including some related discrete dicopper(II) aminoalcoholate derivatives $[Cu_2(H_2tea)_2(ba)_2]\cdot 2H_2O$ (15% yield) {H_3tea, triethanolamine; Hba, benzoic acid}[33a] and $[Cu_2(Hbdea)_2(mba)_2]\cdot 2H_2O$ (18% yield) {H_2bdea, *N*-butyldiethanolamine; Hmba, 4-methylbenzoic acid}.[33b] Better activity of **1**−**3** can thus be regarded to the presence of an increased number of copper centers, their cumulative action, as well as higher stability of the catalytically active multicopper species derived from the parent precatalysts.

To get some information about such possible catalytically active species, we investigated by ESI-MS(±) technique (including the MS/MS studies of the parent fragments) the most active precatalyst **1** before and after its treatment with a nitric acid promoter and hydrogen peroxide oxidant, using the conditions typical to those of catalytic tests. Hence, in addition to the $[Cu_5(Hdmea)_4(pma)(H_2O)_3]^+$ (m/z = 977) and $[Cu_3(Hdmea)_4(pma)]^+$ (m/z = 797) fragments that were present in the ESI-MS(+) spectrum of the parent compound **1**, the ESI-MS(+) plot of the **1**/HNO_3/H_2O_2 system reveals many new peaks, namely $[Cu_5(Hdmea)_4(pma)_2]^+$ (m/z = 1173), $[Cu_4(Hdmea)_4(pma)\ (Hpma)]^+$ (m/z = 1111), $[Cu_3(Hdmea)_4(pma)(H_3pma)]^+$ (m/z = 1050), $[Cu_6(dmea)_4(H_3pma)]^+$ (m/z = 987), and $[Cu_5(dmea)_3(H_2pma)(H_2O)_2]^+$ (m/z = 869). Similarly, a few new rather intense signals also appeared in the ESI-MS(−) plot of **1** after the treatment with HNO_3 and H_2O_2, corresponding to the $[Cu_3(Hdmea)_4(pma)(Hpma)(H_2O)]^-$ (m/z = 1065), $[Cu_5(dmea)_4(pma)(H_2O)]^-$ (m/z = 937), and $[Cu_3(dmea)_4(Hpma)(H_2O)]^-$ (m/z = 811) fragments with expected isotopic distribution patterns. Various ions were selected and subjected to the MS/MS study, which indicated that the heaviest $[Cu_5(Hdmea)_4(pma)_2]^+$ (m/z = 1173) and $[Cu_4(dmea)_4(pma)(H_3pma)]^-$ (m/z = 1109) fragments can be considered as the most relevant parent ions in positive and negative ESI modes, respectively. For these and other peaks, the fragmentation pathways including the MS^2 and, in some cases, MS^3 and MS^4 experiments have been established (see the Supporting Information). These data suggest that upon dissolution and in the course of catalytic reactions the coordination network of **1** partially disaggregates to generate a series of different high-molecular-weight tetracopper and/or pentacopper blocks bearing both amino-alcohol and pyromellitate ligands. Although, because of the complexity of mass spectrometry patterns, it is not evident which of these fragments can potentially constitute the catalytically active species in the present alkane oxidation reactions, we would like to speculate that such species are most likely $[Cu_x(dmea)_4(pma)_y(H_2O)_z]$ {x = 4 or 5; y = 1 or 2, z = 0 or 1}, given some similarities in fragmentation patterns and typical peaks observed in both positive and negative ESI modes and also by considering the relative peak intensities and data of MS/MS studies. The Cu-containing peroxo species have not been detected, although a possibility of their formation at initial stages of catalytic reactions cannot be excluded.[4,28]

In order to understand the nature of oxidizing species involved, we studied the oxidation of linear and branched alkanes and measured the corresponding bond selectivity, regioselectivity, and stereoselectivity parameters (Table 3) in the presence of all three precatalysts. Oxidation of *n*-heptane proceeds without a specific preference to any secondary carbon atom of the hydrocarbon chain. The oxidation of methylcyclohexane and adamantane results in a moderate bond selectivity, suggesting that the tertiary C atom is oxidized with some preference over the secondary C atoms. The oxidations of both *cis*- or *trans*-1,2-dimethylcyclohexane proceed in a nonstereoselective manner, as confirmed by the *trans*/*cis* ratios of 0.6−0.9 between the generated isomeric tertiary alcohols with the mutual *trans* and *cis* orientation of the methyl groups. A partial inversion of the configuration was also detected, with the *cis* isomers being predominant products in both *cis*- and *trans*-1,2-dimethylcyclohexane oxidations.

Table 3. Selectivity Parameters in the Oxidation of Linear and Branched Alkanes[a]

	precatalyst **1**	precatalyst **2**	precatalyst **3**
Regioselectivity			
C(1):C(2):C(3):C(4)[b] (*n*-C_7H_{16})	1:4:4:4	1:5:5:5	1:4:4:4
Bond Selectivity			
1°:2°:3° (methylcyclohexane)[c]	1:5:16	1:5:13	1:5:23
3°/2° (adamantane)[d]	3.4	3.4	3.3
Stereoselectivity			
trans/*cis* (*cis*-dimethylcyclohexane)[e]	0.6	0.7	0.8
trans/*cis* (*trans*-dimethylcyclohexane)[e]	0.9	0.8	0.8

[a]Reaction conditions: precatalyst **1**−**3** (0.005 mmol), TFA (0.05 mmol), alkane (1.0 mmol), H_2O_2 (5.0 mmol), MeCN up to 2.5 mL total volume, 3 h, 50 °C. All parameters were calculated based on the ratios of isomeric alcohols. The calculated parameters were normalized, i.e., recalculated taking into account the number of H atoms at each C atom. [b]Parameters C(1):C(2):C(3):C(4) are the relative reactivities of H atoms at carbons 1, 2, 3, and 4 of the *n*-heptane chain. [c]Parameters 1°:2°:3° are the relative normalized reactivities of the hydrogen atoms at primary, secondary, and tertiary C atoms of methylcyclohexane. [d]Parameters 3°/2° are the relative normalized reactivities of the hydrogen atoms at tertiary and secondary C atoms of adamantane, determined as the ratio of the formed tertiary and secondary alcohol isomers. [e]Parameter *trans*/*cis* is determined as the ratio of the formed tertiary alcohol isomers with mutual *trans* and *cis* orientation of the methyl groups.

The obtained bond selectivity, regioselectivity, and stereoselectivity parameters (Table 3) are indicative of a powerful and rather indiscriminate oxidizing species.[34] Moreover, these selectivity parameters are similar to those reported earlier for other copper-containing catalytic systems operating with $HO^\bullet$ radicals.[4,8a,b,25,28] Therefore, based on the selectivity parameters in the oxidation of linear and branched alkanes, as well as on some kinetic data in the oxidation of cyclohexane, we can propose a general free-radical mechanism undergoing with the participation of hydroxyl radicals as principal oxidizing species. These are formed from H_2O_2 via an interaction with a Cu precatalyst. Then, the hydroxyl radicals abstract H atoms from an alkane forming the alkyl radicals $R^\bullet$, which further react with O_2 (e.g., from air or via partial H_2O_2 decomposition) resulting in the $ROO^\bullet$ radicals that are then transformed to alkyl hydroperoxides ROOH as primary intermediate products.

DOI: 10.1021/acs.inorgchem.5b01983
Inorg. Chem. XXXX, XXX, XXX−XXX

However, alkyl hydroperoxides decompose (conceivably by Cu-catalyzed processes and additionally after the treatment by PPh_3) to furnish the corresponding alcohols and ketones as final oxidation products.[8a,b,25]

CONCLUSIONS

In the present study, we have further explored the application of a versatile aqueous medium self-assembly synthetic protocol toward the generation of a novel series of mixed-ligand 2D coordination polymers **1**−**3**, derived from three different aminoalcohols as main building blocks and pyromellitic acid as a linker. The work thus opens up the application of simple and commercially available aminoalcohols, namely, *N*-ethyldiethanolamine and *N*-benzylethanolamine, as versatile *N,O*-ligands for the construction of coordination polymers. The structural and topological features, water solubility and catalytic behavior of **1**−**3** appear to be dependent on the type of aminoalcohol building block used.

In fact, despite possessing resembling metal−organic 2D layers with the **sql** topology, the coordination networks of **1**−**3** are built from distinct dinuclear or mononuclear copper(II) aminoalcoholate SBUs and μ_4-pyromellitate spacers. Besides, the 2D → 3D extension of metal−organic networks by means of intermolecular hydrogen bonds has been observed in **1** and **2**, furnishing 3D supramolecular nets with a rare **3,4,8T9** or unprecedented topology, respectively, thus contributing to the identification of novel topological motifs.

An interesting feature of **1**−**3** consists in their water solubility, thus opening up the application of these CPs as precatalysts in homogeneous catalytic reactions that proceed in an aqueous medium. Indeed, compounds **1**−**3** act as highly efficient precatalysts for the mild oxidation, by aqueous H_2O_2 in acidic MeCN/H_2O medium, of various cycloalkanes to the corresponding alcohols and ketones, resulting in up to 45% overall product yields in the case of cyclohexane oxidation. In contrast to the oxidation of more reactive substrates than alkanes (e.g., olefins, alcohols), the obtained herein product yields can be rated as very high in the field of alkane oxidation, especially considering the high inertness of these hydrocarbons and the very mild reaction conditions that were applied.[4,15,27−35] A diversity of reaction parameters has been investigated, including the type of precatalyst, the type of acid promoter, substrate scope, relative amounts of reagents and different selectivity parameters. The obtained compounds can also be considered as bioinspired oxidation precatalysts with some potential relevance to the catalytic function of particulate methane monooxygenase. This enzyme comprises a multicopper active site with a *N,O*-environment, which is capable of hydroxylating alkanes.[36,37]

Moreover, a remarkable feature of the present catalytic systems concerns an unusual promoting role of water. Although water typically plays a strongly inhibiting role in mild alkane oxidations (e.g., due to the reduction of the H_2O_2 concentration and lowering of the alkane solubility), we have found a very pronounced promoting behavior of H_2O when using precatalyst **1** and, to a lesser extent, precatalyst **2**. For example, an initial reaction rate (W_0) in the cyclohexane oxidation by the **1**/TFA/H_2O_2 system can be increased from ∼6 × 10^{-8} to ∼93 × 10^{-8} M s^{-1} (∼15-fold growth) upon changing the amount of H_2O in the reaction mixture from ∼4 M to 17.2 M (Figure 8), respectively, followed by a total yield growth from 24% to 45%. We believe that such a highly promoting behavior of water should deserve further exploration and can also be of potential practical significance, namely, permitting the use of diluted, *in situ*-generated aqueous solutions of H_2O_2 as oxidant. Further research to widen both synthetic and catalytic directions toward the design of new copper(II) aminoalcoholate metal−organic networks and their exploration in oxidation catalysis will be pursued.

ASSOCIATED CONTENT

Supporting Information

The Supporting Information is available free of charge on the ACS Publications website at DOI: 10.1021/acs.inorgchem.5b01983.

Materials and methods; additional details on ESI-MS studies; EPR (Figure S1) and UV-vis (Figure S2) spectra; TGA plots (Figures S3−S5); additional structural representations (Figures S6 and S7); and catalytic results (Figures S8−S13) (PDF)

Crystallographic file for $C_{13}H_{27}Cu_2N_2O_9$ (**1**) (CCDC File No. 1419236) (CIF)

Crystallographic file for $C_{17}H_{29}Cu_2N_2O_{10}$ (**2**) (CCDC File No. 1419237) (CIF)

Crystallographic file for $C_{23}H_{28}CuN_2O_7$ (**3**) (CCDC File No. 1419238) (CIF)

AUTHOR INFORMATION

Corresponding Authors

*E-mail: kirillova@ist.utl.pt (M. V. Kirillova).

*E-mail: kirillov@ist.utl.pt (A. M. Kirillov).

Notes

The authors declare no competing financial interest.

ACKNOWLEDGMENTS

This work was supported by the Foundation for Science and Technology (FCT) (Project Nos. IF/01395/2013/CP1163/CT005, PTDC/QUI-QUI/121526/2010, RECI/QEQ-QIN/0189/2012, UID/QUI/00100/2013, SFRH/BPD/78854/2011, and REM 2013), Portugal. We thank Dr. M. C. Oliveira and Ms. A. Dias for ESI-MS(±) measurements.

REFERENCES

(1) For selected books, see: (a) *Metal-Organic Framework Materials*; MacGillivray, L. R., Lukehart, C. M., Eds.; John Wiley & Sons: Chichester, U.K., 2014. (b) *Metal-Organic Frameworks: Applications from Catalysis to Gas Storage*; Farrusseng, D., Ed.; Wiley: Weinheim, Germany, 2011. (c) *Functional Metal-Organic Frameworks: Gas Storage, Separation and Catalysis*; Schroder, M., Ed.; Springer: Berlin, Heidelberg, Germany, 2010.

(2) (a) *Bio- and Bioinspired Nanomaterials*, Ruiz-Molina, D.; Novio, F.; Roscini, C., Eds.; John Wiley & Sons: Weinheim, Germany, 2014. (b) Banerjee, R.; Sahoo, S. C.; Kundu, T. U.S. Patent Appl. 2014/0330020 A1, 2014.

(3) (a) Horcajada, P.; Gref, R.; Baati, T.; Allan, P. K.; Maurin, G.; Couvreur, P.; Ferey, G.; Morris, R. E.; Serre, C. *Chem. Rev.* **2012**, *112*, 1232. (b) McKinlay, A. C.; Morris, R. E.; Horcajada, P.; Ferey, G.; Gref, R.; Couvreur, P.; Serre, C. *Angew. Chem., Int. Ed.* **2010**, *49*, 6260.

(4) Kirillov, A. M.; Kirillova, M. V.; Pombeiro, A. J. L. *Coord. Chem. Rev.* **2012**, *256*, 2741.

(5) For reviews, see: (a) Singh, A.; Mehrotra, R. C. *Coord. Chem. Rev.* **2004**, *248*, 101. (b) Verkade, J. G. *Acc. Chem. Res.* **1993**, *26*, 483.

(6) (a) See: *Cambridge Structural Database (CSD, version 5.36)*; Cambridge Crystallographic Data Centre: Cambridge, U.K., 2015. (b) Allen, F. H. *Acta Crystallogr., Sect. B: Struct. Sci.* **2002**, *B58*, 380.

(7) (a) Kirillov, A. M.; Kirillova, M. V.; Shul'pina, L. S.; Figiel, P. J.; Gruenwald, K. R.; Guedes da Silva, M. F. C.; Haukka, M.; Pombeiro,

DOI: 10.1021/acs.inorgchem.5b01983
Inorg. Chem. XXXX, XXX, XXX−XXX

A. J. L.; Shul'pin, G. B. *J. Mol. Catal. A: Chem.* **2011**, *350*, 26. (b) Figiel, P. J.; Kirillov, A. M.; Guedes da Silva, M. F. C.; Lasri, J.; Pombeiro, A. J. L. *Dalton Trans.* **2010**, *39*, 9879. (c) Wilberger, R.; Piotrowski, H.; Mayer, P.; Vogt, M.; Lorenz, I.-P. *Inorg. Chem. Commun.* **2003**, *6*, 845.
(8) (a) Dias, S. S. P.; Kirillova, M. V.; André, V.; Kłak, J.; Kirillov, A. M. *Inorg. Chem.* **2015**, *54*, 5204. (b) Dias, S. S. P.; Kirillova, M. V.; André, V.; Kłak, J.; Kirillov, A. M. *Inorg. Chem. Front.* **2015**, *2*, 525. (c) Dias, S. S. P.; André, V.; Kłak, J.; Duarte, M. T.; Kirillov, A. M. *Cryst. Growth Des.* **2014**, *14*, 3398.
(9) *APEX2*; Bruker Analytical Systems: Madison, WI, 2005.
(10) Altomare, A.; Burla, M. C.; Camalli, M.; Cascarano, G. L.; Giacovazzo, C.; Guagliardi, A.; Moliterni, A. G. G.; Polidori, G.; Spagna, R. *J. Appl. Crystallogr.* **1999**, *32*, 115.
(11) Sheldrick, G. M. *Acta Crystallogr., Sect. A: Found. Crystallogr.* **2008**, *A64*, 112.
(12) Farrugia, L. J. *J. Appl. Crystallogr.* **1999**, *32*, 837.
(13) (a) Blatov, V. A.; Shevchenko, A. P.; Proserpio, D. M. *Cryst. Growth Des.* **2014**, *14*, 3576. (b) Blatov, V. A. *IUCr CompComm Newsl.* **2006**, *7*, 4.
(14) Spek, A. L. *Acta Crystallogr., Sect. D: Biol. Crystallogr.* **2009**, *D65*, 148.
(15) (a) Shul'pin, G. B. *J. Mol. Catal. A: Chem.* **2002**, *189*, 39. (b) Shul'pin, G. B. *C. R. Chim.* **2003**, *6*, 163. (c) Shul'pin, G. B. *Mini-Rev. Org. Chem.* **2009**, *6*, 95.
(16) (a) Clegg, W.; Holcroft, J. M.; Martin, N. C. *CrystEngComm* **2015**, *17*, 2857. (b) Diaz-Gallifa, P.; Fabelo, O.; Canadillas-Delgado, L.; Pasan, J.; Labrador, A.; Lloret, F.; Julve, M.; Ruiz-Perez, C. *Cryst. Growth Des.* **2013**, *13*, 4735. (c) Zhang, Y.-Y.; Zhao, H.; Yang, E.-C.; Liu, Z.-Y.; Shang, Q.; Zhao, X.-J. *Dalton Trans.* **2015**, *44*, 5826.
(17) (a) Kirillov, A. M.; Karabach, Y. Y.; Kirillova, M. V.; Haukka, M.; Pombeiro, A. J. L. *Cryst. Growth Des.* **2012**, *12*, 1069. (b) Karabach, Y. Y.; Kirillov, A. M.; Haukka, M.; Sanchiz, J.; Kopylovich, M. N.; Pombeiro, A. J. L. *Cryst. Growth Des.* **2008**, *8*, 4100.
(18) (a) Hathaway, B. J. In *Comprehensive Coordination Chemistry*, Vol. 5; Wilkinson, G., Gill, R. D., McCleverty, J. A., Eds.; Pergamon Press: Oxford, U.K., 1987. (b) Hathaway, B. J. *J. Chem. Soc., Dalton Trans.* **1972**, 1196. (c) Elliott, H.; Hathaway, B. J.; Slade, R. C. *J. Chem. Soc. A* **1966**, 1443. (d) Procter, I. M.; Hathaway, B. J.; Nicholls, P. *J. Chem. Soc. A* **1968**, 1678.
(19) Mabbs, F. E.; Collison, D. *Electron Paramagnetic Resonance of d Transition Metal Compounds*; Elsevier Science: Amsterdam, 1992.
(20) Pilbrow, J. R. *Transition Ion Electron Paramagnetic Resonance*; Clarendon Press: Oxford, U.K., 1990.
(21) (a) Lever, A. B. P. *Inorganic Electronic Spectroscopy*; Elsevier: Amsterdam, 1968. (b) Eryazici, I.; Moorefield, C. N.; Newkome, G. R. *Chem. Rev.* **2008**, *108*, 1834.
(22) (a) Yang, L.; Powell, D. R.; Houser, R. P. *Dalton Trans.* **2007**, 955. (b) Addison, A. W.; Rao, T. N.; Reedijk, J.; van Rijn, J.; Verschoor, G. C. *J. Chem. Soc., Dalton Trans.* **1984**, 1349.
(23) (a) Zolotarev, P. N.; Arshad, M. N.; Asiri, A. M.; Al-Amshany, Z. M.; Blatov, V. A. *Cryst. Growth Des.* **2014**, *14*, 1938. (b) Baburin, I. A.; Blatov, V. A.; Carlucci, L.; Ciani, G.; Proserpio, D. M. *Cryst. Growth Des.* **2008**, *8*, 519.
(24) (a) *The Reticular Chemistry Structure Resource (RCSR) Database*; available via the Internet at: www.rcsr.net. (b) O'Keeffe, M.; Peskov, M. A.; Ramsden, S. J.; Yaghi, O. M. *Acc. Chem. Res.* **2008**, *41*, 1782.
(25) Kirillov, A. M.; Kirillova, M. V.; Pombeiro, A. J. L. *Adv. Inorg. Chem.* **2013**, *65*, 1.
(26) (a) Kirillova, M. V.; Kirillov, A. M.; Martins, A. N. C.; Graiff, C.; Tiripicchio, A.; Pombeiro, A. J. L. *Inorg. Chem.* **2012**, *51*, 5224. (b) Kirillov, A. M.; Coelho, J. A. S.; Kirillova, M. V.; Guedes da Silva, M. F. C.; Nesterov, D. S.; Gruenwald, K. R.; Haukka, M.; Pombeiro, A. J. L. *Inorg. Chem.* **2010**, *49*, 6390.
(27) Schuchardt, U.; Cardoso, D.; Sercheli, R.; Pereira, R.; da Cruz, R. S.; Guerreiro, M. C.; Mandelli, D.; Spinace, E. V.; Pires, E. L. *Appl. Catal., A* **2001**, *211*, 1.
(28) (a) Kirillova, M. V.; Kirillov, A. M.; Mandelli, D.; Carvalho, W. A.; Pombeiro, A. J. L.; Shul'pin, G. B. *J. Catal.* **2010**, *272*, 9. (b) Kirillova, M. V.; Kozlov, Y. N.; Shul'pina, L. S.; Lyakin, O. Y.; Kirillov, A. M.; Talsi, E. P.; Pombeiro, A. J. L.; Shul'pin, G. B. *J. Catal.* **2009**, *268*, 26.
(29) Kirillov, A. M.; Shul'pin, G. B. *Coord. Chem. Rev.* **2013**, *257*, 732.
(30) Kirillov, A. M.; Haukka, M.; Guedes da Silva, M. F. C.; Pombeiro, A. J. L. *Eur. J. Inorg. Chem.* **2005**, *2005*, 2071.
(31) (a) Kirillova, M. V.; Kirillov, A. M.; Pombeiro, A. J. L. *Chem.—Eur. J.* **2010**, *16*, 9485. (b) Kirillova, M. V.; Kirillov, A. M.; Kuznetsov, M. L.; Silva, J. A. L.; Frausto da Silva, J. J. R.; Pombeiro, A. J. L. *Chem. Commun.* **2009**, 2353. (c) Kirillova, M. V.; Kirillov, A. M.; Pombeiro, A. J. L. *Adv. Synth. Catal.* **2009**, *351*, 2936.
(32) (a) Kirillova, M. V.; Kuznetsov, M. L.; Romakh, V. B.; Shul'pina, L. S.; Fraústo da Silva, J. J. R.; Pombeiro, A. J. L.; Shul'pin, G. B. *J. Catal.* **2009**, *267*, 140. (b) Kuznetsov, M. L.; Pombeiro, A. J. L. *Inorg. Chem.* **2009**, *48*, 307.
(33) (a) Kirillov, A. M.; Kopylovich, M. N.; Kirillova, M. V.; Karabach, E. Y.; Haukka, M.; da Silva, M. F. C. G.; Pombeiro, A. J. L. *Adv. Synth. Catal.* **2006**, *348*, 159. (b) Gruenwald, K. R.; Kirillov, A. M.; Haukka, M.; Sanchiz, J.; Pombeiro, A. J. L. *Dalton Trans.* **2009**, 2109.
(34) (a) Shul'pin, G. B. *Dalton Trans.* **2013**, *42*, 12794. (b) Shul'pin, G. B. *Org. Biomol. Chem.* **2010**, *8*, 4217.
(35) *Ullmann's Encyclopedia of Industrial Chemistry*, 6th Edition; Wiley–VCH: Weinheim, Germany, 1999–2013.
(36) Lieberman, R. L.; Rosenzweig, A. C. *Nature* **2005**, *434*, 177.
(37) Himes, R. A.; Karlin, K. D. *Curr. Opin. Chem. Biol.* **2009**, *13*, 119.

DOI: 10.1021/acs.inorgchem.5b01983
Inorg. Chem. XXXX, XXX, XXX–XXX